SCIENCE CHINA
Information Sciences

• RESEARCH PAPER •

December 2016, Vol. 59 122902:1–122902:13
doi: 10.1007/s11432-016-0582-y

Quaternion-based robust trajectory tracking control for uncertain quadrotors

Tianpeng HE[1], Hao LIU[2*] & Shu LI[1]

[1]*School of Aeronautic Science and Engineering, Beihang University, Beijing* 100191*, China;*
[2]*School of Astronautics, Beihang University, Beijing* 100191*, China*

Received August 30, 2016; accepted September 28, 2016; published online November 4, 2016

Abstract This paper presents a robust nonlinear controller design approach for uncertain quadrotors to implement trajectory tracking missions. The quaternion representation is applied to describe the rotational dynamics in order to avoid the singularity problem existing in the Euler angle representation. A nonlinear robust controller is proposed, which consists of an attitude controller to stabilize the rotational motions and a position controller to control translational motions. The quadrotor dynamics involves uncertainties such as parameter uncertainties, nonlinearities, and external disturbances and their effects on closed-loop control system can be guaranteed to be restrained. Simulation results on the quadrotor demonstrate the effectiveness of the designed control approach.

Keywords quadrotor, quaternion, trajectory tracking, robust control

Citation He T P, Liu H, Li S. Quaternion-based robust trajectory tracking control for uncertain quadrotors. Sci China Inf Sci, 2016, 59(12): 122902, doi: 10.1007/s11432-016-0582-y

1 Introduction

Unmanned aerial vehicles have attracted much attention in the control and robotics circles as shown in [1–3]. Quadrotors are increasingly popular unmanned aerial vehicle platforms, because of four fixed-pitch rotors instead of complex mechanical control linkages as stated in [4]. Therefore, quadrotors could be widely used in various fields including exploration, surveillance, and inspection. Therefore, these unmanned vehicles have also received much attention in the control scientific circle. Traditional proportional-integral-derivative (PID) control approach [5, 6], nested saturation control method [7], flatness-based control algorithm [8], cascade control scheme by singular perturbation theory [9] were researched to achieve the automatic control of the six degrees of freedom (6DOF) quadrotors. However, the effects of various uncertainties on the closed-loop control systems were not fully discussed in the aforementioned published work.

Actually, the quadrotor dynamics involves multiple uncertainties including parameter perturbations, coupled and nonlinear dynamics, and external unknown disturbances. Therefore, many efforts have been devoted to achieve the robust control of the uncertain quadrotors. In [10, 11], sliding modebased control methods were discussed to achieving robustness properties for quadrotors with a transient estimation

* Corresponding author (email: liuhao13@buaa.edu.cn)

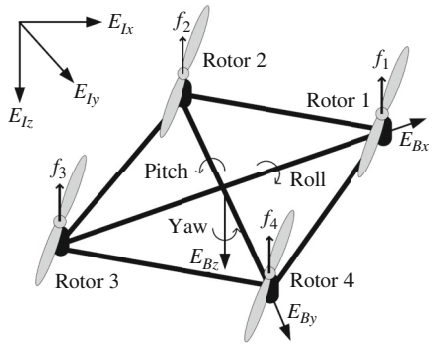

Figure 1 Quadrotor schematic.

process. New types of adaptive control schemes were studied in [12, 13] to achieve the robust tracking performances for uncertain robotic quadrotors. In [14], a robust suboptimal control algorithm was designed by the mixed H_2 and H_∞ performance analysis. However, much previously published work (see, for example, Refs. [3–16]) mainly focused on robust controller design by the Euler angle representation which suffers from the singular problems, as shown in [17].

As shown in [18], quaternion-based representations can be used to avoid the singularity problem in the attitude representation approaches, especial when the aerial vehicles are required to implement aggressive maneuvers. But the quaternion-based representations with a unit length constraint are complicated and thereby it is not easy to design a robust trajectory tracking controller directly on these representations. In [18–20], new developed adaptive controllers were proposed for the quadrotors with nonlinear motion equations described by the quaternions. However, for these proposed adaptive closed-loop systems, their dynamical tracking performances cannot be specified. The nonlinear feedback control laws based on quaternion representations were studied in [17, 21], but the effects of multiple uncertainties on the closed-loop control system were not discussed in the stability analysis. Other kinds of control methods were discussed in [22–25]. The controllers by sliding mode method are good choices to achieve asymptotic tracking properties for the quadrotors. In [26], a sliding mode observer was introduced with filters to reduce chattering. In [27], a non-smooth controller by the sliding mode approach was designed to stabilize the quadrotor dynamics. Furthermore, in [28], a smooth nonlinear controller was proposed with a comparatively long transient process for uncertain quadrotors.

In this paper, a quaternion-based robust nonlinear control method is proposed to achieve the trajectory tracking control for 6DOF uncertain robotic quadrotors. The designed trajectory tracking controller consists of an attitude controller and a position controller. The attitude controller is employed to stabilize the rotational motion, while the position controller to control translational motions. Compared to previous studies on the robust control problem for quadrotors involving uncertainties, the influences of various uncertainties on the closed-loop control system can be restrained and the singular problem in the attitude presentations can be avoided. Besides, the proposed control scheme leads to a smooth control law.

The following parts of the current paper are organized as follows: in Section 2, the translational and rotational motions of the quadrotor are briefly described by nonlinear equations based on the unit quaternion representations; in Section 3, a new robust trajectory tracking controller is proposed for the uncertain quadrotor and the robust tracking performances of the closed-loop control system are discussed. Simulation results are given in Section 4 and Section 5 concludes the whole work of this paper.

2 Quadrotor model

As depicted in Figure 1, the quadrotor is an aerial robotic unmanned vehicle equipped with four rotors powered by electronic motors. Let $E_I = \{E_{Ix}, E_{Iy}, E_{Iz}\}$ and $E_B = \{E_{Bx}, E_{By}, E_{Bz}\}$ denote an inertial frame and a frame attached to the quadrotor body. Let the vectors $p_I = [\,p_{Ix}\ p_{Iy}\ p_{Iz}\,]^{\mathrm{T}}$ and $v_I =$

$[\, v_{Ix}\ v_{Iy}\ v_{Iz}\,]^{\mathrm{T}}$ be the position and translational velocity of the vehicle mass center expressed in the frame E_I, respectively. Let $\omega_B = [\, \omega_{Bx}\ \omega_{By}\ \omega_{Bz}\,]^{\mathrm{T}}$ be the angular velocity depicted in the frame E_B. The following mathematical equations can be obtained to describe the translational and rotational motions of the 6DOF quadrotor (see, for example, Ref. [20])

$$\begin{aligned} &\dot{p}_I = v_I,\\ &m\dot{v}_I = Rf_B + d_f,\\ &\dot{R} = RS(\omega_B),\\ &J\dot{\omega}_B = -S(\omega_B)J\omega_B + \tau_B + d_\tau, \end{aligned} \tag{1}$$

where m, J, f_B, τ_B, and $R \in SO(3)$ represent the vehicle mass, the inertia tensor of the quadrotor body, the external force and torque acting on quadrotor in the frame E_B, the rotational matrix mapping vectors expressed in the frame E_B into the vectors expressed in the frame E_I. J is a symmetric and positive definite constant matrix and $d_f = [d_{fi}]_{3\times 1}$ and $d_\tau = [d_{\tau i}]_{3\times 1}$ are external bounded and continuously differentiable disturbances, and

$$S(\omega_B) = \begin{bmatrix} 0 & -\omega_{Bz} & \omega_{By}\\ \omega_{Bz} & 0 & -\omega_{Bx}\\ -\omega_{By} & \omega_{Bx} & 0 \end{bmatrix}.$$

Four unit quaternions are applied to describe the rotational motion here. Let $q = [\, q_0\ \bar{q}_1^{\mathrm{T}}\,]^{\mathrm{T}}$ be the four unit quaternions, and q_0 and $\bar{q}_1 = [\, q_1\ q_2\ q_3\,]^{\mathrm{T}}$ indicate the quaternion scalar and vector parts of the unit quaternions. q_0 and $\bar{q}_1$ satisfy the constraint: $q_0^2 + \|\bar{q}_1\|_2^2 = 1$. $R = [R_{ij}]_{3\times 3}$ can be expressed by the following unit quaternion representations (see, Ref. [20] to mention a few)

$$R = \begin{bmatrix} 1-2q_2^2-2q_3^2 & 2q_1q_2-2q_0q_3 & 2q_1q_3+2q_0q_2\\ 2q_1q_2+2q_0q_3 & 1-2q_1^2-2q_3^2 & 2q_2q_3-2q_0q_1\\ 2q_1q_3-2q_0q_2 & 2q_2q_3+2q_0q_1 & 1-2q_1^2-2q_2^2 \end{bmatrix}.$$

It follows that the quaternion propagation equations can be expressed without any nonlinear uncertain terms as follows

$$\begin{aligned} &\dot{q}_0 = -0.5\bar{q}_1^{\mathrm{T}}\omega_B,\\ &\dot{\bar{q}}_1 = 0.5\,[q_0 I_3 + S(\bar{q}_1)]\,\omega_B, \end{aligned} \tag{2}$$

where I_n is an $n\times n$ unit matrix. The external force $f_B = [f_{Bx}\, f_{By}\, f_{Bz}]^{\mathrm{T}}$ and torque $\tau_B = [\tau_{Bx}\, \tau_{By}\, \tau_{Bz}]^{\mathrm{T}}$ for the quadrotor are different from those acting on the regular helicopters. τ_{Bx}, τ_{By}, and τ_{Bz} are torques around e_{Bx}, e_{By}, and e_{Bz} and can be obtained by the following expressions

$$\begin{aligned} &\tau_{Bx} = l_{rc}(f_2 - f_4),\\ &\tau_{By} = l_{rc}(f_1 - f_3),\\ &\tau_{Bz} = k_{fm}(f_1 - f_2 + f_3 - f_4), \end{aligned} \tag{3}$$

where $l_{rc} > 0$ and $k_{fm} > 0$ indicate the distance from each rotor to the mass center and the scaling constant, and f_i $(i = 1, 2, 3, 4)$ are the lift thrusts produced by the four rotors respectively. f_B can be given as follows

$$f_B = \begin{bmatrix} 0\\ 0\\ -f_T \end{bmatrix} + R^{\mathrm{T}} \begin{bmatrix} 0\\ 0\\ mg \end{bmatrix},$$

where $f_T = \sum_{i=1}^{4} f_i$ and g is the gravitational constant. The lift thrusts f_i $(i = 1, 2, 3, 4)$ can be given by

$$f_i = k_{f\omega}\omega_{ri}^2, \quad i = 1, 2, 3, 4, \tag{4}$$

where ω_{ri} $(i = 1, 2, 3, 4)$ are the rotational velocities of each rotor, and $k_{f\omega}$ is a positive constant. Design the control inputs u_i $(i = 1, 2, 3, 4)$ as

$$\begin{aligned} u_1 &= \omega_{r1}^2 + \omega_{r2}^2 + \omega_{r3}^2 + \omega_{r4}^2, \\ u_2 &= \omega_{r2}^2 - \omega_{r4}^2, \\ u_3 &= \omega_{r1}^2 - \omega_{r3}^2, \\ u_4 &= \omega_{r1}^2 - \omega_{r2}^2 + \omega_{r3}^2 - \omega_{r4}^2. \end{aligned} \tag{5}$$

Remark 1. From (2), one can see that quaternion propagation equations are nonlinear. The advantage of the quaternion-based representations is that the singularity problem in the attitude representation approaches can be avoided, especially when the quadrotors implement aggressive maneuvers. However, the disadvantage is that the quaternion-based representations with a unit length constraint are complicated, which leads to difficulties in designing a robust trajectory tracking controller directly on these representations. Since the quadrotor is aimed to implement the aggressive maneuvers, the quaternion-based representations are used instead of the Euler angle based representations here.

In this paper, the outputs are selected as: the longitudinal position p_{Ix}, the lateral position p_{Iy}, and the vertical position p_{Iz} and their desired references are denoted by p_{Ix}^r, p_{Iy}^r, and p_{Iz}^r, respectively. Let $p_I^r = [\, p_{Ix}^r \;\; p_{Iy}^r \;\; p_{Iz}^r \,]^{\mathrm{T}}$. These desired references and their derivatives are assumed to be piecewise uniformly bounded. The position tracking error is defined as $e_p = [e_{pi}]_{3\times 1} = p_I - p_I^r$. Define the translational velocity tracking error $e_v = [e_{vi}]_{3\times 1}$ as

$$e_v = \dot{e}_p = v_I - v_I^r, \tag{6}$$

where $v_I^r = [\, v_{Ix}^r \;\; v_{Iy}^r \;\; v_{Iz}^r \,]^{\mathrm{T}}$ are the desired translational velocity. Let $a_{f1} = 2/m$, $a_{f2} = 2/m$, and $a_{f3} = k_{f\omega}/m$. From the second equation in (1), one can obtain

$$\begin{aligned} \dot{e}_{v1} &= -a_{f1}^N(q_1q_3 + q_0q_2)f_T + \Delta_{f1}, \\ \dot{e}_{v2} &= -a_{f2}^N(q_2q_3 - q_0q_1)f_T + \Delta_{f2}, \\ \dot{e}_{v3} &= -a_{f3}^N(1 - 2q_1^2 - 2q_2^2)u_1 + \Delta_{f3}, \end{aligned} \tag{7}$$

where

$$\begin{aligned} \Delta_{f1} &= -a_{f1}^{\Delta}(q_1q_3 + q_0q_2)f_T - \ddot{p}_{Ix}^r + d_{f1}, \\ \Delta_{f2} &= -a_{f2}^{\Delta}(q_2q_3 - q_0q_1)f_T - \ddot{p}_{Iy}^r + d_{f2}, \\ \Delta_{f3} &= -a_{f3}^{\Delta}(1 - 2q_1^2 - 2q_2^2)u_1 - \ddot{p}_{Iz}^r + d_{f3}. \end{aligned} \tag{8}$$

In this paper, the superscript N is used to stand for the nominal values of parameters and the superscript Δ for the parameter uncertainties satisfying $a_{fi} = a_{fi}^N + a_{fi}^{\Delta}$. It can be seen that a_{fi}^N $(i = 1, 2, 3)$ are positive and a_{fi}^N $(i = 1, 2, 3)$ are assumed to satisfy $|\Delta a_{fi}| < a_{fi}^N$ $(i = 1, 2, 3)$.

Let $q^r = [\, q_0^r \;\; q_1^r \;\; q_3^r \;\; q_4^r \,]^{\mathrm{T}}$ be the desired attitude references, which are generated based on the longitudinal and lateral position tracking errors and will be discussed in the following controller design section in details. As shown in [18], the attitude tracking error can be given by a nonlinear function $\tilde{Q}(q, q^r)$ as

$$\tilde{Q}(q, q^r) = 2\mathrm{sgn}(q_0^rq_0 + q_1^rq_1 + q_2^rq_2 + q_3^rq_3) \begin{bmatrix} -q_0^rq_1 + q_1^rq_0 + q_2^rq_3 - q_3^rq_2 \\ -q_0^rq_2 - q_1^rq_3 + q_2^rq_0 + q_3^rq_1 \\ -q_0^rq_3 + q_1^rq_2 - q_2^rq_1 + q_3^rq_0 \end{bmatrix}.$$

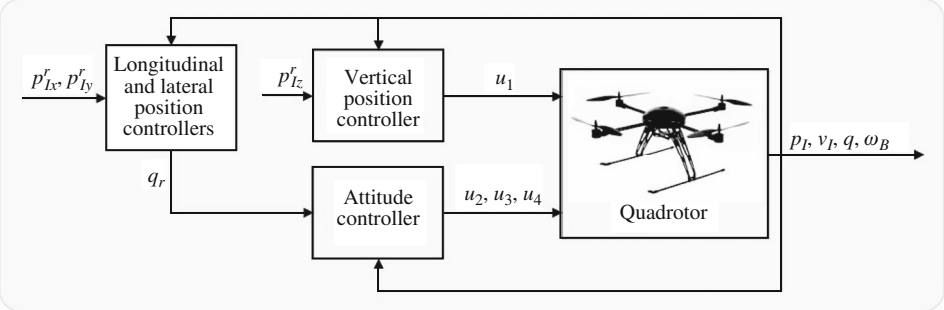

Figure 2 The block diagram of the control system.

Let $e_q = [e_{qi}]_{3\times 1} = \tilde{Q}(q, q^r)$ and $e_\omega = [e_{\omega i}]_{3\times 1} = \omega_B - \omega_B^r$, where ω_b^r represents the desired rotational speeds in the frame E_B. From [18], one can have

$$\dot{e}_q = e_\omega. \tag{9}$$

Let $A_{\tau u} = \mathrm{diag}\,(l_{rc}k_{f\omega}, l_{rc}k_{f\omega}, k_{fm}k_{f\omega})$ and $A_\tau = J^{-1}A_{\tau u}$. Combining the fourth equation in (1) and (3)–(5) yields

$$\dot{e}_\omega = A_\tau^N u_\tau + \Delta_\tau, \tag{10}$$

where $u_\tau = [\,u_2\ u_3\ u_4\,]^{\mathrm{T}}$ and

$$\Delta_\tau = A_\tau^\Delta \tau_B - J^{-1}S(\omega_B)J\omega_B + J^{-1}d_\tau - \dot{\omega}_B^r. \tag{11}$$

A_τ^N is invertible, since the matrix A_τ^N is a symmetric and positive definite matrix. Therefore, one can assume that A_τ^N and A_τ^Δ satisfy the inequality $\|(A_\tau^N)^{-1}A_\tau^\Delta\|_1 < 1$.

Remark 2. Actually, by combining (6), (7), (9), and (10), one can obtain the whole quaternion-based nonlinear model.

The control goal in this paper is to achieve the trajectory tracking of p_{Ix}^r, p_{Iy}^r, and p_{Iz}^r for p_{Ix}, p_{Iy}, and p_{Iz} respectively, while stabilizing the attitude dynamics. All of the errors e_p, e_v, e_q, and e_ω are needed to converge into given neighbourhoods of the origin in a finite time.

3 Robust trajectory tracking controller design

In this section, a robust trajectory tracking controller consisting of a position controller and an attitude controller is designed for a 6DOF uncertain quadrotor. First, the vertical position controller will be designed for the height tracking, followed by the stability analysis in this channel. Second, the longitudinal and lateral position controllers will be designed, followed by the attitude controller design. Last, it will be shown that the longitudinal and lateral position errors and the attitude errors can also ultimately converge into the neighborhood of origin by given bounds. The block diagram of the whole control system is depicted in Figure 2.

3.1 Vertical position controller design

From (6) and (7), the vertical dynamics can be described by the following equation as

$$\ddot{e}_{p3} = -a_{f3}^N(1 - 2q_1^2 - 2q_2^2)u_1 + \Delta_{f3}. \tag{12}$$

Design the preliminary height control law as

$$u_1 = -\frac{-k_{p3}^d\dot{e}_{p3} - k_{p3}^p e_{p3} + v_1}{a_{f3}^N(1 - 2q_1^2 - 2q_2^2)}, \tag{13}$$

where k_{p3}^d and k_{p3}^p are positive constants and v_1 is an additional control input to be defined. Then, the equation describing the vertical dynamics can be rewritten as

$$\ddot{e}_{p3} = -k_{p3}^d \dot{e}_{p3} - k_{p3}^p e_{p3} + v_1 + \Delta_{f3}. \tag{14}$$

From (14), it can be seen that if v_1 is designed to cancel the term Δ_{f3}, it yields the following vertical closed-loop control system

$$\ddot{e}_{p3} + k_{p3}^d \dot{e}_{p3} + k_{p3}^p e_{p3} = 0,$$

which is defined as the nominal vertical closed-loop system here. The tracking performance of the nominal system can be specified by designing the system with desired poles.

Since the uncertainty Δ_{f3} cannot be obtained directly in practical applications, the additional control input v_1 is constructed based on the RCT (robust compensating technique) as shown in [29–31]. The model (14) is a two-dimensional system with relative degree 2, therefore a second order filter $\Phi_{p3}(p)$ is introduced: $\Phi_{p3}(p) = g_{p3}^2/(p+g_{p3})^2$, where p is the Laplace operator and g_{p3} is a positive constant to be determined.

Remark 3. The robust filter has the property, that is, if the robust filter parameter g_{p3} has a sufficiently large value, the filter frequency bandwidth would be sufficiently wide and thus the filter gain would be close to be 1. In this case, more interested signals with low frequency would pass the filter, while more noise with high frequency would be rejected.

Therefore, design the control input v_1 as

$$v_1 = -\Phi_{p3}(p)\Delta_{f3}. \tag{15}$$

Remark 4. One can observe that the additional control input v_1 would get close to $-\Delta_{f3}$ and thereby restrain the influence of Δ_{f3}, if g_{p3} is sufficiently large.

Since Δ_{f3} cannot be measured directly, a good choice is to replace Δ_{f3} in (15) by the vertical tracking error e_{p3}. Actually, from (14) and (15), one can obtain

$$v_1 = -g_{p3}^2 \frac{(p^2 + pk_{p3}^d + k_{p3}^p)e_{p3} - v_1}{(p+g_{p3})^2}.$$

Therefore, in practical applications, the additional control input v_1 can be implemented as

$$v_1 = -\frac{p^2 + pk_{p3}^d + k_{p3}^p}{p^2 + 2pg_{p3}} g_{p3}^2 e_{p3}. \tag{16}$$

Define the vertical position error vector $e_v = [\, e_{p3} \;\; \dot{e}_{p3} \,]$. Then, combining (14) and (15), one can have

$$\dot{e}_v = A_v e_v + B_v(1 - \Phi_{p3})\Delta_{f3}, \tag{17}$$

where

$$A_v = \begin{bmatrix} 0 & 1 \\ -k_{p3}^p & -k_{p3}^d \end{bmatrix}, \quad B_v = \begin{bmatrix} 0 \\ 1 \end{bmatrix}.$$

3.2 Stabilization analysis of the vertical dynamics

The tracking properties of the vertical closed-loop control system can be summarized by the following theorem.

Theorem 1. For a given positive constant ε_v and the given bounded vertical initial tracking error $e_v(0)$, there exist positive constants T_v^* and g_{p3}^*, such that for $g_{p3} > g_{p3}^*$ and $t \geqslant T_v^*$, the vertical position error e_v is bounded and satisfies $|e_v(t)| \leqslant \varepsilon_v$.

Proof. From (14), one can have

$$\|e_v\|_\infty \leqslant \eta_{v(0)} + \delta_v \|\Delta_{f3}\|_\infty, \tag{18}$$

where $\eta_{v(0)} = \sup_{t\geqslant 0} |e^{A_v t} e_v(0)|$, $\delta_v = \|(pI_2 - A_v)^{-1} B_v (1 - \Phi_{p3})\|_1$, and I_n is an $n \times n$ identity matrix. Substituting (13) into (8), one can obtain

$$\Delta_{f3} = -a_{f3}^{\Delta}(k_{p3}^d \dot{e}_{p3} + k_{p3}^p e_{p3})/a_{f3}^N + a_{f3}^{\Delta} v_1 / a_{f3}^N - \ddot{p}_{Iz}^r + d_{f3}.$$

It follows

$$\|\Delta_{f3}\|_\infty \leqslant \pi_{ef3} \|e_v\|_\infty + \rho_{v1} \|v_1\|_\infty + \pi_{cf3}, \tag{19}$$

where ρ_{v1}, π_{ef3}, and π_{cf3} are positive constants satisfying $\rho_{v1} = |a_{f3}^{\Delta}|/a_{f3}^N < 1$, $\pi_{ef3} = \rho_{v1}|k_{p3}^d| + \rho_{v1}|k_{p3}^p|$, and $\pi_{cf3} \geqslant |d_{f3} - \ddot{p}_{Iz}^r|$, respectively. From (15), one can obtain

$$\|v_1\|_\infty \leqslant \|\Delta_{f3}\|_\infty. \tag{20}$$

Combining (19) and (20) leads to

$$\|\Delta_{f3}\|_\infty \leqslant \pi'_{ef3} \|e_v\|_\infty + \pi'_{cf3}, \tag{21}$$

where $\pi'_{ef3} = \pi_{ef3}/(1 - \delta_{v1})$ and $\pi'_{cf3} = \pi_{cf3}/(1 - \delta_{v1})$. If the positive parameter g_{p3} is larger and thus the frequency bandwidth of the filter $\Phi_{p3}(p)$ is wider, the filter gain is more approximate to 1. In this case, one can obtain a positive constant g_{p3}^{*1} such that for $g_{p3} > g_{p3}^{*1}$, $\delta_v < 1/(2\pi'_{ef3})$. In this case, from (19) and (21), one can have

$$\begin{aligned} &\|e_v\|_\infty \leqslant 2\eta_{v(0)} + \pi'_{cf3}/\pi'_{ef3}, \\ &\|\Delta_{f3}\|_\infty \leqslant 2\eta_{v(0)} \pi'_{ef3} + 2\pi'_{cf3}. \end{aligned} \tag{22}$$

From (22), it can be observed that for the given initial state, $\|e_v\|_\infty$ and $\|\Delta_{f3}\|_\infty$ are bounded; that is, there exist positive constants η_{ev} and $\eta_{\Delta f3}$ such that

$$\begin{aligned} &\|e_v\|_\infty \leqslant \eta_{ev}, \\ &\|\Delta_{f3}\|_\infty \leqslant \eta_{\Delta f3}. \end{aligned} \tag{23}$$

Finally, from (14), (15), and (23), one can obtain the following expression as

$$\max_j |e_{v,j}(t)| \leqslant \max_j \left| c_{2,j}^{\mathrm{T}} e^{A_v t} e_z(0) \right| + \delta_v \eta_{\Delta f3}, \tag{24}$$

where $c_{n,j}$ is an $n \times 1$ vector with 1 on the element and 0 elsewhere. Therefore, from (24), it can be seen that for a given positive constant ε_v and the given bounded initial state $e_v(0)$, there exist positive constants T_v^* and $g_{p3}^* \geqslant g_{p3}^{*1}$, such that for $g_{p3} > g_{p3}^*$ and $t \geqslant T_v^*$, e_v satisfies $|e_v(t)| \leqslant \varepsilon_v$.

3.3 Longitudinal and lateral position controller design

From (6) and (7), the longitudinal and lateral dynamics can be described by the following equations as

$$\begin{aligned} \ddot{e}_{p1} &= -a_{f1}^N (q_1 q_3 + q_0 q_2) f_T + \Delta_{f1}, \\ \ddot{e}_{p2} &= -a_{f2}^N (q_2 q_3 - q_0 q_1) f_T + \Delta_{f2}. \end{aligned} \tag{25}$$

Let $u_{p1} = q_1^r q_3^r + q_0^r q_2^r$ and $u_{p2} = q_2^r q_3^r - q_0^r q_1^r$ denote the virtue control inputs for the longitudinal and lateral positions, respectively. Define the preliminary feedback control laws u_{pi} $(i = 1, 2)$ as

$$u_{pi} = -\frac{-k_{pi}^d \dot{e}_{pi} - k_{pi}^p e_{pi} + v_{pi}}{a_{fi}^N f_T}, \quad i = 1, 2, \tag{26}$$

where k_{pi}^d and k_{pi}^p $(i = 1, 2)$ are positive parameters and v_{pi} $(i = 1, 2)$ are additional control inputs to attenuate the influence of Δ'_{fi} $(i = 1, 2)$. Construct v_{pi} $(i = 1, 2)$ with robust filters as follows

$$v_{pi} = -\Phi_{pi}(p) \Delta_{fi}, \quad i = 1, 2, \tag{27}$$

where $\Phi_{pi}(p) = g_{pi}^2/(p + g_{pi})^2$ $(i = 1, 2)$ and g_{pi} $(i = 1, 2)$ are positive parameters to be determined. These additional control inputs can be implemented in a similar way to that in the vertical channel.

3.4 Attitude controller design

In this subsection, the robust controller is designed to achieve the practical tracking of the desired attitude reference q^r for q. Since the yaw angle is required to be stabilized at 0, one can obtain $q_1^r q_2^r + q_0^r q_3^r = 0$ from [32]. From (9) and (10), the attitude dynamics can be described by the following expression

$$\ddot{e}_q = A_\tau^N u_\tau + \Delta_\tau. \tag{28}$$

Let $e_A = [\, e_q^{\mathrm{T}} \;\; e_\omega^{\mathrm{T}} \,]^{\mathrm{T}}$. Design the preliminary attitude control law as

$$u = -(A_\tau^N)^{-1}(K_\tau e_A - v_A), \tag{29}$$

where $K_\tau = \mathrm{diag}(K_\tau^d, K_\tau^p)$, $K_\tau^i = \mathrm{diag}(k_{\tau x}^i, k_{\tau y}^i, k_{\tau z}^i)$ $(i = d, p)$, and v_A is the additional control input to restrain the effects of Δ_τ. $k_{\tau i}^d$ and $k_{\tau i}^p$ $(i = x, y, z)$ are selected to be positive constants. Substituting (29) into (28), one has

$$\ddot{e}_q = -K_\tau^d \dot{e}_q - K_\tau^p e_q + v_A + \Delta_\tau. \tag{30}$$

Similarly with the vertical channel, construct the additional control input v_A as

$$v_A = -\Phi_\tau(p)\Delta_\tau, \tag{31}$$

where $\Phi_\tau(p) = \mathrm{diag}(\Phi_{\tau x}(p), \Phi_{\tau y}(p), \Phi_{\tau z}(p))$, $\Phi_{\tau i}(p) = g_{\tau i}^2/(p + g_{\tau i})^2$ $(i = x, y, z)$, and $g_{\tau i}$ $(i = x, y, z)$ are positive parameters to be determined. v_A can also be implemented in a similar way with v_1 in the vertical channel.

3.5 Stabilization analysis of the longitudinal, lateral, and attitude dynamics

Define the longitudinal and lateral position error vectors $e_{pi} = [\, e_{pi} \;\; \dot{e}_{pi} \,]$ $(i = 1, 2)$. If the decay of the attitude tracking error e_q to 0 is much faster than the convergence of the translational position errors e_{pi} $(i = 1, 2)$ to 0 and thereby the attitude error dynamics can be ignored in the translational dynamics analysis, one can obtain the following expressions by substituting (26) and (27) into (25) as

$$\dot{e}_{pi} = A_{pi} e_{pi} + B_{pi}(1 - \Phi_{pi})\Delta_{fi}, \quad i = 1, 2, \tag{32}$$

where

$$A_{pi} = \begin{bmatrix} 0 & 1 \\ -k_{pi}^p & -k_{pi}^d \end{bmatrix}, \quad B_{pi} = \begin{bmatrix} 0 \\ 1 \end{bmatrix}.$$

The details on how to achieve the condition that the convergence of e_q to 0 is much faster than that of e_q will be discussed at the end of this subsection. Now, the tracking properties of the longitudinal and lateral control systems can be summarized by the following theorem.

Theorem 2. For given positive constants ε_{pi} $(i = 1, 2)$ and the given bounded initial tracking errors e_{pi} $(i = 1, 2)$, there exist positive constants T_{pi}^* and g_{pi}^* $(i = 1, 2)$, such that for $g_{pi} > g_{pi}^*$ and $t \geqslant T_{pi}^*$, the position tracking errors e_{pi} $(i = 1, 2)$ are bounded and satisfy $|e_{pi}(t)| \leqslant \varepsilon_{pi}$ $(i = 1, 2)$.

Theorem 2 can be proven by a similar way to Theorem 1. Therefore, there also exist positive constants η_{epi} and $\eta_{\Delta fi}$ $(i = 1, 2)$, such that

$$\begin{aligned} &\|e_{pi}\|_\infty \leqslant \eta_{epi}, \\ &\|\Delta_{fi}\|_\infty \leqslant \eta_{\Delta fi}, \quad i = 1, 2. \end{aligned} \tag{33}$$

Let $e_\tau = [\, e_q^{\mathrm{T}} \;\; \dot{e}_q^{\mathrm{T}} \,]^{\mathrm{T}}$. From (30) and (31), one can have

$$\dot{e}_\tau = A_\tau e_\tau + B_\tau(I_3 - \Phi_\tau)\Delta_\tau, \tag{34}$$

where

$$A_\tau = \begin{bmatrix} 0 & I_3 \\ -K_\tau^p & -K_\tau^d \end{bmatrix}, \quad B_\tau = \begin{bmatrix} 0 \\ I_3 \end{bmatrix}.$$

The robustness properties of the closed-loop attitude control system can be summarized as follows.

Theorem 3. For a given positive constant ε_τ and the given bounded initial tracking error $e_\tau(0)$, there exist positive constants T_τ^* and $g_{\tau i}^*$ $(i = x, y, z)$, such that for $g_{\tau i} > g_{\tau i}^*$ and $t \geqslant T_\tau^*$, the attitude tracking error e_τ is bounded and satisfies $|e_\tau(t)| \leqslant \varepsilon_\tau$.

Proof. From (34), one can have

$$\|e_\tau\|_\infty \leqslant \eta_{\tau(0)} + \delta_\tau \|\Delta_\tau\|_\infty, \tag{35}$$

where $\eta_{\tau(0)} = \sup_{t\geqslant 0} |e^{A_\tau t} e_\tau(0)|$ and $\delta_\tau = \|(pI_6 - A_\tau)^{-1} B_\tau (I_3 - \Phi_\tau)\|_\infty$. Similarly to Theorem 1, there exist positive constants $\pi_{e\tau 1}$, $\pi_{e\tau 2}$, and $\pi_{c\tau}$ such that

$$\|\Delta_\tau\|_\infty \leqslant \pi_{e\tau 1} \|e_\tau\|_\infty + \pi_{e\tau 2} \|e_\tau\|_\infty^2 + \pi_{c\tau}. \tag{36}$$

If the following inequalities hold

$$(\sqrt{\delta_\tau} + \delta_\tau)^{-1} \geqslant \pi_{e\tau 1} + \pi_{e\tau 2} \|e_\tau\|_\infty, \tag{37}$$

from (35) and (36), one obtains

$$\|\Delta_\tau\|_\infty \leqslant \sqrt{\delta_\tau^{-1}} \eta_{\tau(0)} + (1 + \sqrt{\delta_\tau}) \pi_{c\tau}. \tag{38}$$

In this case, combining (35) and (38), one has

$$\|e_\tau\|_\infty \leqslant \eta_{\tau(0)} + \sqrt{\delta_\tau}(\eta_{\tau(0)} + \sqrt{\delta_\tau} \pi_{c\tau} + \delta_\tau \pi_{c\tau}). \tag{39}$$

From the above expression, it can be seen that the tracking error e_τ is bounded. Actually, the inequality (37) results in the attractive region of e_τ as

$$\left\{ e_\tau : \|e_\tau\|_\infty \leqslant \pi_{e\tau 2}^{-1} (\sqrt{\delta_\tau} + \delta_\tau)^{-1} - \pi_{e\tau 2}^{-1} \pi_{e\tau 1} \right\}. \tag{40}$$

It can be observed that there exist positive constants $g_{\tau i}^{*1}$ $(i = x, y, z)$, such that for $g_{\tau i} > g_{\tau i}^{*1}$, the following inequalities hold

$$\begin{aligned} &\|e_\tau(0)\|_\infty \leqslant \pi_{e\tau 2}^{-1} (\sqrt{\delta_\tau} + \delta_\tau)^{-1} - \pi_{e\tau 2}^{-1} \pi_{e\tau 1}, \\ &\eta_{\tau(0)} + \sqrt{\delta_\tau}(\eta_{\tau(0)} + \sqrt{\delta_\tau} \pi'_{c\tau} + \delta_\tau \pi'_{c\tau}) \leqslant \pi_{e\tau 2}^{-1} (\sqrt{\delta_\tau} + \delta_\tau)^{-1} - \pi_{e\tau 2}^{-1} \pi_{e\tau 1}, \end{aligned} \tag{41}$$

then e_τ can remain inside this attractive region and thus (40) holds. In this case, from (34) and (38), one can obtain

$$\max_j |e_{\tau,j}| \leqslant \max_l \left| c_{6,j}^{\mathrm{T}} e^{A_\tau t} e_\tau(0) \right| + \sqrt{\delta_\tau}(\eta_{\tau(0)} + \sqrt{\delta_\tau} \pi_{c\tau} + \delta_\tau \pi_{c\tau}). \tag{42}$$

Therefore, it can be seen from the above inequality that, for a given positive constant ε_τ and a given initial state $e_\tau(0)$, there exist positive constants T_τ^* and $g_{\tau i}^*$ $(i = x, y, z)$, such that for $g_{\tau i} > g_{\tau i}^* \geqslant g_{\tau i}^{*1}$, the attitude tracking error e_τ is bounded and satisfies $\max_j |e_{\tau,j}| \leqslant \varepsilon_\tau, \forall t \geqslant T_\tau^*$.

4 Simulation results

In this section, the vehicle is required to track the sine wave references with approximate 20 deg. amplitude for the three positions, simultaneously. The helicopter nominal parameters are selected as (standard

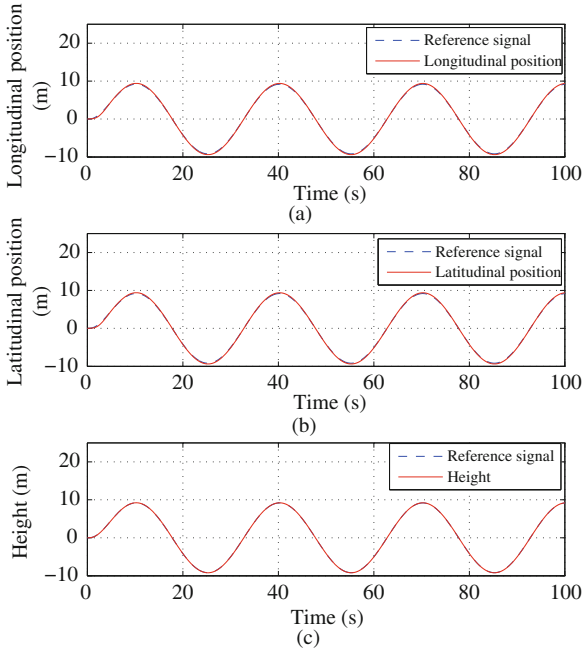

Figure 3 (Color online) Position responses with RCT. (a) Longitudinal response; (b) latitudinal response; (c) height response.

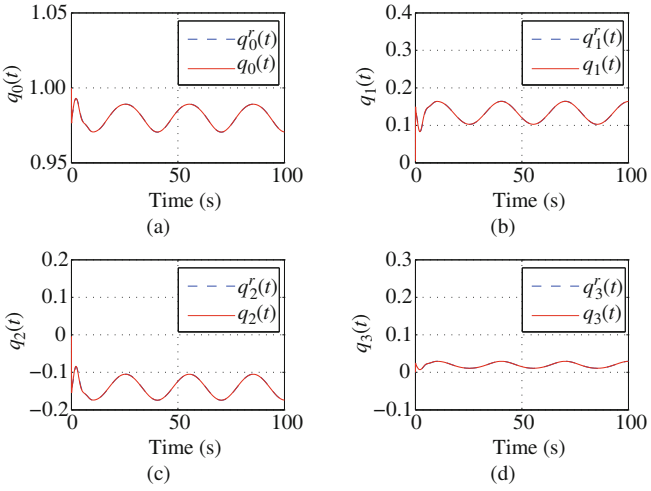

Figure 4 (Color online) Attitude responses with RCT. (a) Response of $q_0(t)$; (b) response of $q_1(t)$; (c) response of $q_2(t)$; (d) response of $q_3(t)$.

unit): $m^N = 2$, $J^N = \mathrm{diag}(1.25, 1.25, 2.5)$, $l_{rc}^N = 0.2$, and $k_{fm}^N = 1$. The robust controller parameters are selected as: $k_{p1}^p = 2$, $k_{p2}^p = 2$, $k_{p3}^p = 10$, $k_{p1}^d = 1$, $k_{p2}^d = 1$, $k_{p3}^d = 25$, $k_{\tau x}^p = 20$, $k_{\tau y}^p = 20$, $k_{\tau z}^p = 10$, $k_{\tau x}^d = 100$, $k_{\tau y}^d = 100$, $k_{\tau z}^d = 25$, $g_{p1} = 50$, $g_{p2} = 50$, $g_{p3} = 50$, $g_{\tau x} = 500$, $g_{\tau y} = 500$, and $g_{\tau z} = 100$. Vehicle parameters are assumed to be 40% larger than the nominal parameters, and quadrotor is subject to external bounded disturbances as: $d_{\tau 1} = 0.2\sin(t)$, $d_{\tau 2} = 0.2\sin(t)$, $d_{\tau 3} = 0.2\sin(t)$, $d_{f1} = 0.2\sin(t)$, $d_{f2} = 0.2\sin(t)$, and $d_{f3} = \sin(t)$.

The unmanned vehicle starts from $p_I(0) = (0, 0, 0)$ and p_{Ix}, p_{Iy}, and p_{Iz} are needed to track p_{Ix}^r, p_{Iy}^r, and p_{Iz}^r, respectively. The position responses and attitude responses are depicted in Figure 3 and Figure 4, respectively. In contrast, the corresponding attitude and position responses without the RCT are given in Figure 5 and Figure 6, respectively. Position tracking errors and attitude errors are compared in Figure 7 and Figure 8, respectively. It can be observed that the tracking errors are improved especially in the longitudinal and latitudinal position channel by the additive inputs based on the RCT.

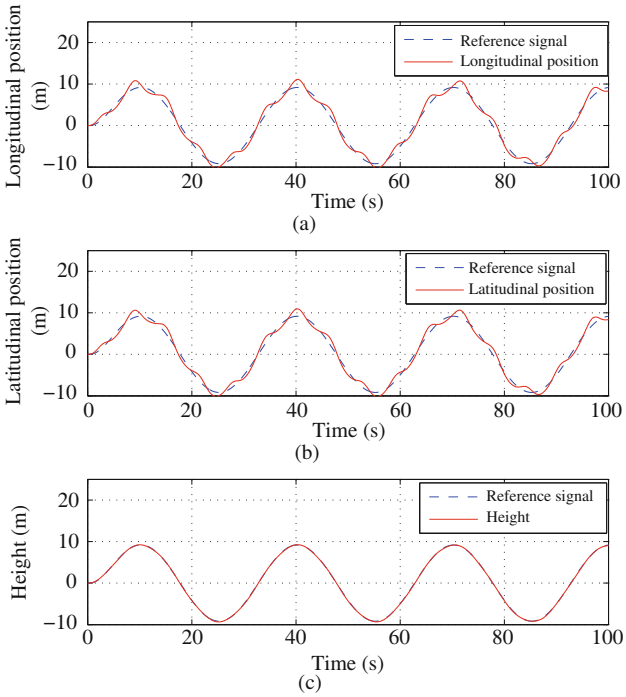

Figure 5 (Color online) Position responses without RCT. (a) Longitudinal response; (b) latitudinal response; (c) height response.

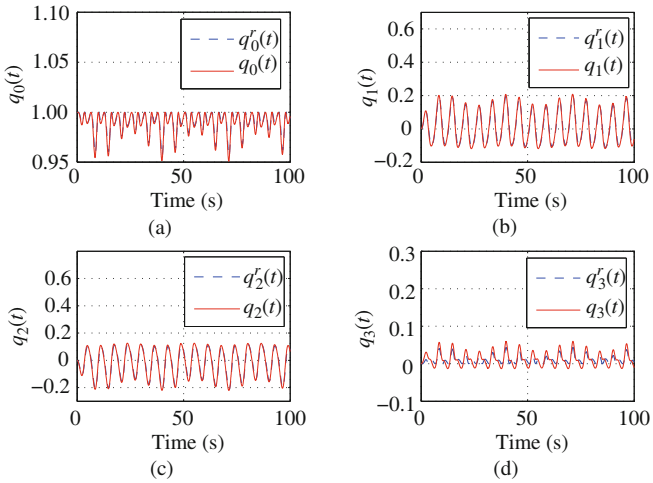

Figure 6 (Color online) Attitude responses without RCT. (a) Response of $q_0(t)$; (b) response of $q_1(t)$; (c) response of $q_2(t)$; (d) response of $q_3(t)$.

5 Conclusion

Robust trajectory tracking control was achieved for uncertain quadrotors based on the unit quaternion representations to avoid the singularity problem. A robust nonlinear controller was constructed consisting of an attitude controller and a position controller. Although the quadrotor is subject to parameter uncertainties, nonlinearities, and external disturbances, the tracking errors of the closed-loop system are proven to converge into given neighborhoods of the origin ultimately. Simulation results demonstrated the effectiveness of the designed control method.

This paper only presents the simulation results for the proposed closed-loop control system. The designed robust control approach will be implemented in the quadrotor experimental platform to validate its advantages.

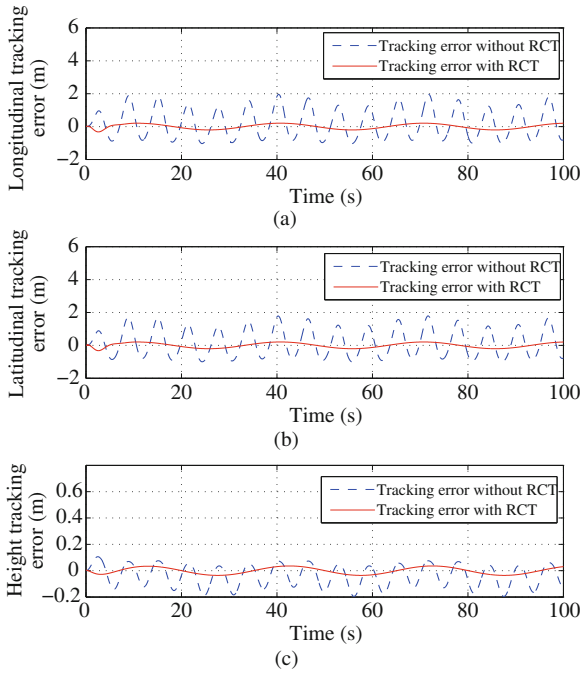

Figure 7 (Color online) Position tracking error comparison. (a) Tracking error in the longitudinal channel; (b) tracking error in the latitudinal channel; (c) tracking error in the height channel.

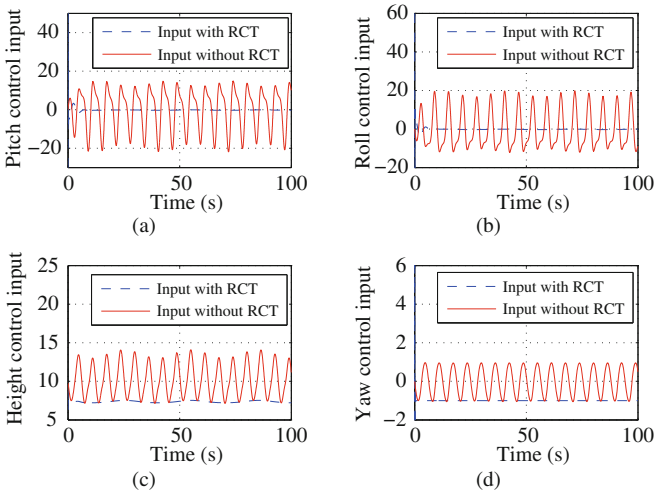

Figure 8 (Color online) Control inputs. (a) Control inputs in the pitch channel; (b) control inputs in the roll channel; (c) control inputs in the height channel; (d) control inputs in the yaw channel.

Acknowledgements This work was supported by National High-Tech R&D Program of China (863 Program) (Grant No. 2012AA112201) and National Natural Science Foundation of China (Grant No. 61503012).

Conflict of interest The authors declare that they have no conflict of interest.

References

1 Hoffmann G M, Huang H, Waslander S L. Precision flight control for a multi-vehicle quadrotor helicopter testbed. Control Eng Pract, 2011, 19: 1023–1036
2 Sun C H, Duan H B. Markov decision evolutionary game theoretic learning for cooperative sensing of unmanned aerial vehicles. Sci China Technol Sci, 2015, 58: 1392–1400
3 Tang S, Yang Q H, Qian S K, et al. Height and attitude active disturbance rejection controller design of a small-scale helicopter. Sci China Inf Sci, 2015, 58: 032202

4 Alexis K, Nikolakopoulos G, Tzes A. Switching model predictive attitude control for a quadrotor helicopter subject to atmosphere disturbances. Control Eng Pract, 2011, 10: 1195–1207
5 Pounds P, Mahony R, Corke P. Modelling and control of a large quadrotor robot. Control Eng Pract, 2010, 18: 691–699
6 Mahony R, Kumar V, Corke P. Multirotor aerial vehicles: modeling, estimation, and control of quadrotor. IEEE Robot Automat Mag, 2012, 19: 20–32
7 Castillo P, Dzul A, Lozano R. Real-time stabilization and tracking of a four-rotor mini rotorcraft. IEEE Trans Control Syst Technol, 2004, 12: 510–516
8 Aguilar-Ibanez C, Sira-Ramirez H, Suarez-Castanon S, et al. The trajectory tracking problem for an unmanned four-rotor system: flatness-based approach. Int J Control, 2012, 85: 69–77
9 Bertrand S, Guenard N, Hamel T, et al. A hierarchical controller for miniature VTOL UAVs: design and stability analysis using singular perturbation theory. Control Eng Pract, 2011, 19: 1099–1108
10 Besnard L, Shtessel Y B, Landrum B. Quadrotor vehicle control via sliding mode controller driven by sliding mode disturbance observer. J Franklin Inst, 2012, 349: 658–684
11 Luque-Vega L, Castillo-Toledo B, Loukianov A G. Robust block second order sliding mode control for a quadrotor. J Franklin Inst, 2012, 349: 719–739
12 Dydek Z T, Annaswamy A M, Lavretsky E. Adaptive control of quadrotor UAVs: a design trade study with flight evaluations. IEEE Trans Control Syst Technol, 2013, 21: 1400–1406
13 Zuo Z Y. Trajectory tracking control design with command-filtered compensation for a quadrotor. IET Control Theory Appl, 2010, 11: 2343–2355
14 Ryan T, Kim H J. LMI-based gain synthesis for simple robust quadrotor control. IEEE Trans Automat Sci Eng, 2013, 10: 1173–1178
15 Liu H, Li D J, Xi J X, et al. Robust attitude controller design for miniature quadrotors. Int J Robust Nonlinear Control, 2016, 26: 681–696
16 Liu H, Lu G, Zhong Y S. Robust LQR attitude control of a 3-DOF lab helicopter for aggressive maneuvers. IEEE Trans Ind Electron, 2013, 60: 4627–4636
17 Tayebi A, McGilvray S. Attitude stabilization of a VTOL quadrotor aircraft. IEEE Trans Control Syst Technol, 2006, 14: 562–571
18 Johnson E N, Kannan S K. Adaptive trajectory control for autonomous helicopters. J Guid Control Dyn, 2005, 28: 524–538
19 Zhang R, Quan Q, Cai K Y. Attitude control of a quadrotor aircraft subject to a class of time-varying disturbances. IET Control Theory Appl, 2011, 5: 1140–1146
20 Isidori A, Marconi L, Serrani A. Robust nonlinear motion control of a helicopter. IEEE Trans Automat Control, 2003, 48: 413–426
21 Guerrero-Castellanos J F, Marchand N, Hably A, et al. Bounded attitude control of rigid bodies: real-time experimentation to a quadrotor mini-helicopter. Control Eng Pract, 2011, 19: 790–797
22 Li K B, Chen L, Tang G L. Algebraic solution of differential geometric guidance command and time delay control. Scie China Technol Sci, 2015, 58: 565–573
23 Guo S P, Li D X, Meng Y H, et al. Task space control of free-floating space robots using constrained adaptive RBF-NTSM. Sci China Technol Sci, 2014, 57: 828–837
24 Shen Y Y, Wang Y Q, Liu M L, et al. Acquisition algorithm assisted by AGC control voltage for DSSS signals. Sci China Technolog Sci, 2015, 58: 2195–2206
25 Wang H X, Wang W Y, Zheng Y H. Bifurcation analysis for Hindmarsh-Rose neuronal model with time-delayed feedback control and application to chaos control. Sci China Technol Sci, 2014, 57: 872–878
26 Derafa L, Benallegue A, Fridman L. Super twisting control algorithm for the attitude tracking of a four rotors UAV. J Franklin Inst, 2012, 349: 685–699
27 Xu R, Ozguner U. Sliding mode control of a class of underactuated systems. Automatica, 2008, 44: 233–241
28 Zhao B, Xian B, Zhang Y, et al. Nonlinear robust sliding mode control of a quadrotor unmanned aerial vehicle based on immersion and invariance method. Int J Robust Nonlinear Control, 2015, 18: 3714–3731
29 Liu H, Li D J, Zuo Z Y, et al. Robust three-loop trajectory tracking control for quadrotors with multiple uncertainties. IEEE Trans Ind Electron, 2016, 63: 2263–2274
30 Liu H, Wang X F, Zhong Y S. Quaternion-based robust attitude control for uncertain robotic quadrotors. IEEE Trans Ind Inform, 2015, 11: 406–415
31 Liu H, Zhao W B, Zuo Z Y, et al. Robust control for quadrotors with multiple time-varying uncertainties and delays. IEEE Trans Ind Electron, 2016, doi: 10.1109/TIE.2016.2612618
32 Stevens B L, Lewis F L. Aircraft Control and Simulation. New Jersey: John Wiley & Sons, Inc., 2003